



# Exploring the Structure, Electron Density and HOMO-LUMO Studies of Tetrathiafulvalene (TTF) as Organic Superconductors: A DFT and AIM Analysis

Research Article

P. Gnanamozi<sup>1</sup>, V. Pandiyan<sup>1</sup>, P. Srinivasan<sup>2,\*</sup> and A. David Stephen<sup>3</sup>

<sup>1</sup>Department of Physics, Nehru Memorial College, Puthanampatti 621007, India

<sup>2</sup>PG & Research Department of Physics, Chikkaiah Naicker College, Erode 638004, India

<sup>3</sup>Department of Physics, Sri Shakthi institute of Engineering Technology, Coimbatore 641062, India

\*Corresponding author: [sriniscience@gmail.com](mailto:sriniscience@gmail.com)

**Abstract.** The Structure, Electron density and HOMO-LUMO analysis of TTF molecule was carefully evaluated by *ab initio* (HF) and density functional theory (B3LYP) calculations. The optimized (HF/6-311G\*\* and B3LYP/6-311G\*\*, B3LYP/auf-cc-PVDZ) geometric parameters are in excellent agreement with the similar type experimental data. For both levels of calculation, the low charge accumulation have C–S and C≡N bonds, at the bond critical point, which gives that the bond charges are highly depleted compared with all other bonds in the molecule. Further, AIM theory shows the difference of charge distribution in all bonds. The molecular conductivity (HOMO-LUMO gap) properties are solely related to the ESP of the entire system. The ionization potential gives the very good information of conductivity. These observations give an insight on this kind of super conducting material, which are useful to design navel electronic devices.

**Keywords.** TTF; DFT; Electron density; Energy gap and ESP

**PACS.** 71.20.-b; 73.20.At; 98.38.Am

**Received:** February 19, 2019

**Accepted:** March 12, 2019

Copyright © 2019 P. Gnanamozi, V. Pandiyan, P. Srinivasan and A. David Stephen. *This is an open access article distributed under the Creative Commons Attribution License, which permits unrestricted use, distribution, and reproduction in any medium, provided the original work is properly cited.*

## 1. Introduction

The processing characteristics of organic superconductors make them potentially useful for electronic applications where low-cost, large area coverage, and structural flexibility are required [15]. Charge carrier mobility is a measure of the quality of organic superconductors and is a primary factor that determines the performance of organic field effect transistors (OFETs) [6, 11]. The highest mobilities are found in single crystals due to molecular ordering that permits good overlapping of the  $\pi$ - $\pi$  orbitals. A mobility of  $1.5 \text{ cm}^2/\text{Vs}$  was reported for pentacene [6] and recently a mobility of  $8 \text{ cm}^2/\text{Vs}$  was reported for rubrene [9, 13]. To progress in this field toward device applications, it is very important to search for new molecules that are able to act as organic superconductors [5] and also to develop easier methods to grow single crystals or films.

In recent years, the Tetrathiafulvalene (TTF) and its derivatives are successfully used as building blocks for charge-transfer salts, giving rise to a multitude of organic conductors and superconductors [7]. These conducting salts are prepared mainly as single crystals but also as thin films of nano crystals supported on dielectric polymers [4, 17]. The driving force in the crystallization of the salts is the  $\pi$ - $\pi$  stacking, which permits, together with the S...S interactions, an intermolecular electronic transfer responsible for their transport properties. The transport properties of a few single crystals of neutral TTF derivatives have been measured, showing a semiconductor character with room temperature, conductivity on the order of  $10^{-5} \text{ S/cm}$  [14]. Additionally, organic thin films of TTF derivatives have been grown by vacuum deposition techniques, but only their morphology and nano mechanical properties have been studied [23]. However, TTF derivatives have never been used for the preparation of OFETs despite the fact that they are soluble in various solvents, easily chemically modified and good electron donors. In the present study, we have undertaken Tetrathiafulvalene [7] (TTF) super conducting molecule (Figure 1) is to understand its bonding nature and to relate the topological properties of its bonds and the molecular orbital energy gap using *ab initio* density functional theory.

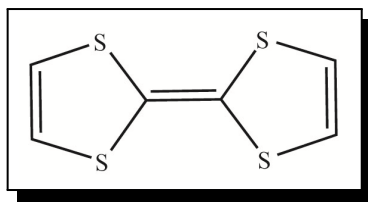


**Figure 1.** Chemical Structure of Tetrathiafulvalene (TTF) molecule

The topological properties of the bonds such as electron density, its gradient vector field  $\nabla\rho(r)$  and its Laplacian of electron density  $\nabla^2\rho_{bcP}(r)$  reveal the nature of the bonds between the atoms in molecules (AIM) [1, 3]. The atomic interactions are largely contributed by that pair of gradient lines in the  $\nabla\rho(r)$  field that originates from the critical saddle point between two neighbouring atoms, and terminates at the two neighbouring nuclei, along which the electron density is maximum with respect to any other line. These lines are the atomic interaction line, which is the bond path in an equilibrium system. Invariably, we obtained a  $(3, -1)$  type of bond critical points (bcps), for all bonds in the molecule. In the  $(3, -1)$  bcp, the rank 3 can be found from three non-zero eigenvalues and the signature  $-1$ , from the sum of algebraic signs of the

same.  $\nabla^2\rho_{bcp}(r) > 0$  for the closed-shell interaction i.e., non-covalent atomic interaction [26]. Thus,  $\nabla^2\rho_{bcp}(r)$  characterizes the type of atomic interactions.

## 2. Computational Details

To obtain the exact geometry and the electronic parameters of the TTF molecule, a minimum energy structure optimization was carried out from the HF and B3LYP level of theories with the basis sets 6-311G\*\* [19] and *aug-cc-PVDZ* [29] using Gaussian03 program [10]. The optimization of DFT method converged at threshold limits of 0.000057 and 0.001692 au for the maximum force and displacement, respectively. The electron density [ $\rho_{bcp}(r)$ ], eigen values [ $\lambda_1, \lambda_2, \lambda_3$ ], bond ellipticity ( $\epsilon$ ) and the electrostatic properties has been calculated from the wave function obtained from the above methods using AIM theory [2], implemented in AIMPAC program suite [12]. The deformation density of the molecule was plotted by *wfn2plots* and *XDGRAPH* [28]. The *3D plot* software [27] was used to generate the ESP map of the molecule.

## 3. Results and Discussion

### 3.1 Structural Aspects

Figure 2 shows the ball and stick model of energy minimized geometry of Tetrathiafulvalene (TTF) molecule. The structural parameters of the molecule such as bond lengths, bond angles, and torsion angles were calculated from the 6-311G\*\* and *aug-cc-PVDZ* basis sets.

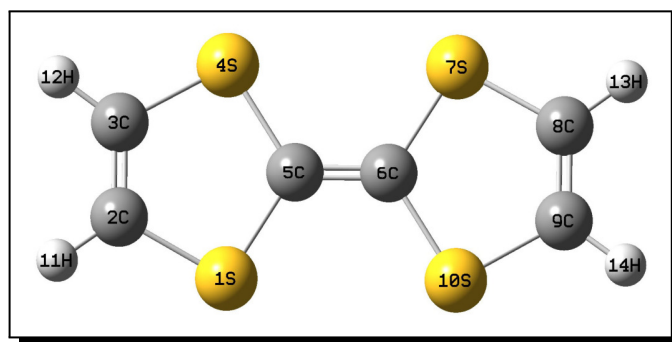


**Figure 2.** The optimized structure of TTF molecule at B3LYP/*aug-cc-PVDZ* level

Careful examination of the geometrical parameters, specifically, the bond distances predicted by HF/6-311G\*\* and B3LYP/6-311G\*\* methods were found to be consistently shorter than the B3LYP/*aug-cc-PVDZ* method (Table 1). The C–C bond lengths calculated from B3LYP/6-311G\*\* method is 1.333 Å, which is slightly longer than the bond distance predicted by B3LYP/*aug-cc-PVDZ* and the difference is 0.07 Å. Notably, the C–S distances [C(2)–S(1): 1.763 Å; C(5)–S(1): 1.786 Å] found by B3LYP/6-311G\*\* is significantly shorter than the B3LYP/*aug-cc-PVDZ* and predicted values [C(2)–S(1): 1.766 Å; C(5)–S(1): 1.791 Å], and it is slightly longer when compared with the reported value 1.758 Å [8]. This difference is attributed to the different methods of computation. The C–H bond distances calculated from both levels of calculations are ranged 1.081–1.088 Å, respectively. The C–S–C bond angles predicted from B3LYP/6-311G\*\* and B3LYP/*aug-cc-PVDZ* methods (Table 1) are found to be almost equal and the average value is 94.7°.

**Table 1.** Geometric parameters of TTF molecule (Å, °)

Bonds	HF/6-311G**	B3LYP/6-311G**	B3LYP/Aug-cc-PVDZ
<b>Bond length (Å)</b>			
C(2)–S(1)	1.758	1.763	1.766
C(5)–S(1)	1.777	1.786	1.791
C(2)–C(3)	1.314	1.333	1.34
C(2)–H(11)	1.072	1.081	1.088
C(3)–S(4)	1.758	1.763	1.766
C(3)–H(12)	1.072	1.081	1.088
C(5)–S(4)	1.777	1.786	1.791
C(5)–C(6)	1.324	1.346	1.353
C(6)–S(7)	1.777	1.786	1.791
C(6)–S(10)	1.777	1.786	1.791
C(8)–S(7)	1.758	1.763	1.766
C(8)–C(9)	1.314	1.333	1.34
C(8)–H(13)	1.072	1.081	1.088
C(9)–S(10)	1.758	1.763	1.766
C(9)–H(14)	1.072	1.081	1.088
<b>Bond angle (°)</b>			
C(2)–S(1)–C(5)	95.1	94.7	94.9
S(1)–C(2)–C(3)	118.2	118	118.1
S(1)–C(2)–H(11)	117.1	116.9	117.1
C(3)–C(2)–H(11)	124.7	125	124.8
C(2)–C(3)–S(4)	118.2	118	118.1
C(2)–C(3)–H(12)	124.7	125.1	124.8
S(4)–C(3)–H(12)	117.1	116.9	117.1
C(3)–S(4)–C(5)	95.1	94.7	94.8
S(1)–C(5)–S(4)	113.5	113.6	113.9
S(1)–C(5)–C(6)	123.2	123.2	123.1
S(4)–C(5)–C(6)	123.2	123.2	123.1
C(5)–C(6)–S(7)	123.2	123.2	123.1
C(5)–C(6)–S(10)	123.2	123.2	123.1
S(7)–C(6)–S(10)	113.5	113.6	113.9
C(6)–S(7)–C(8)	95.1	94.7	94.9
S(7)–C(8)–C(9)	118.2	118	118.1
S(7)–C(8)–H(13)	117.1	116.9	117.1
C(9)–C(8)–H(13)	124.7	125	124.8
C(8)–C(9)–S(10)	118.2	118	118.1
C(8)–C(9)–H(14)	124.7	125.1	124.8
S(10)–C(9)–H(14)	117.1	116.9	117.1
C(6)–S(10)–C(9)	95.1	94.7	94.8
<b>Torsion angle (°)</b>			
C(5)–S(1)–C(2)–C(3)	0.0	6	3.4
C(5)–S(1)–C(2)–H(11)	180.0	-175.4	-177.3
C(2)–S(1)–C(5)–S(4)	0.0	-9.7	-5.6
C(2)–S(1)–C(5)–C(6)	-180.0	170.5	175.1
S(1)–C(2)–C(3)–S(4)	0.0	0	0
S(1)–C(2)–C(3)–H(12)	-180.0	178.5	179.2
H(11)–C(2)–C(3)–S(4)	180.0	-178.5	-179.2
H(11)–C(2)–C(3)–H(12)	0.0	0	0
C(2)–C(3)–S(4)–C(5)	0.0	-6	-3.4
H(12)–C(3)–S(4)–C(5)	-180.0	175.4	177.3
C(3)–S(4)–C(5)–S(1)	0.0	9.7	5.6
C(3)–S(4)–C(5)–C(6)	180.0	-170.5	-175.1
S(1)–C(5)–C(6)–S(7)	-180.0	179.8	179.3
S(1)–C(5)–C(6)–S(10)	0.0	0	0
S(4)–C(5)–C(6)–S(7)	0.0	0	0
S(4)–C(5)–C(6)–S(10)	180.0	-179.8	-179.3
C(5)–C(6)–S(7)–C(8)	-180.0	170.5	175.1
S(10)–C(6)–S(7)–C(8)	0.0	-9.7	-5.6
C(5)–C(6)–S(10)–C(9)	180.0	-170.5	-175.1
S(7)–C(6)–S(10)–C(9)	0.0	9.7	5.6
C(6)–S(7)–C(8)–C(9)	0.0	6	3.4
C(6)–S(7)–C(8)–H(13)	180.0	-175.4	-177.3
S(7)–C(8)–C(9)–S(10)	0.0	0	0
S(7)–C(8)–C(9)–H(14)	180.0	178.5	179.2
H(13)–C(8)–C(9)–S(10)	-179.0	-178.5	-179.2
H(13)–C(8)–C(9)–H(14)	0.0	0	0
C(8)–C(9)–S(10)–C(6)	0.0	-6	-3.4
H(14)–C(9)–S(10)–C(6)	-180.0	175.4	177.3

### 3.2 Electron Density Analysis

Figure 3, depicts the deformation density of the molecule calculated from the wave function acquired from DFT calculation. The deformation density map gives the a spherical nature of the electron density of atoms in molecules, which allows visualizing the areas of charge accumulation in the bonding regions and the lone pair positions of atoms in molecules [1]. The TTF molecule (Figure 3) deformation density shows, the covalent nature of bonds from the area of electron density distribution of the molecule. While, the S–C bonds exhibit covalent bond nature, its electron density distribution is not similar to the other bonding regions of the molecule; the map clearly differentiates the dissimilarity of electron density distribution of various bonding regions of the molecule (Figure 3).

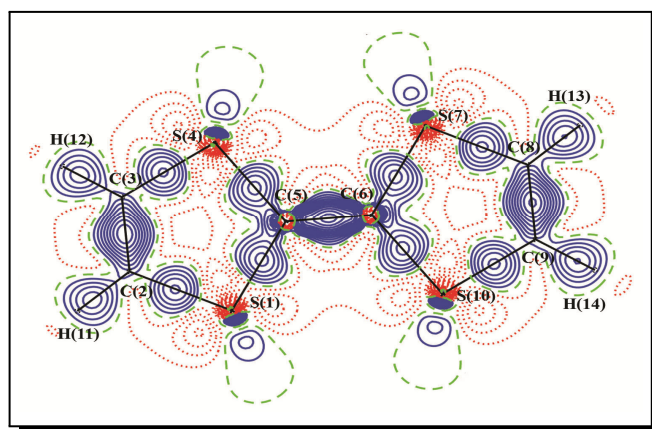


**Figure 3.** Deformation density in the plane of the molecule. The solid lines (blue) are positive, dashed (red) are negative and dotted lines are zero contours. Contour intervals are drawn at  $0.05 \text{ e}\text{\AA}^{-3}$

Notably, the charge accumulation in C(3)–C(2) [ $2.23 \text{ e}\text{\AA}^{-3}$ ] bond is slightly lower than the C(6)–C(5) bond [ $\sim 2.17 \text{ e}\text{\AA}^{-3}$ ] of the TTF molecule (Table 2). Further, the C–S bond density ranges from  $\sim 1.27$  to  $1.33 \text{ e}\text{\AA}^{-3}$ , this is found to be significantly lower than the C–C bonds in the molecule, and the low  $\rho_{bc_p}(r)$  of C–S bond is due to the effect of neighbouring atoms in the molecule. The very less values of electron density gives the charges of these bonds are not well localized in the bonding region (Table 2).

**Table 2.** Bond topological properties of TTF molecule

Bonds	$\rho_{bc_p}(r)^a$	$\epsilon^c$	$\lambda_1$	$\lambda_2$	$\lambda_3$	$d_1^d$	$d_2^d$	$D^d$
C(5)–S(1)	1.27	0.20	-6.5	-5.4	3.5	1.792	0.890	0.902
C(2)–S(1)	1.33	0.21	-7.1	-5.8	3.4	1.766	0.901	0.865
C(3)–C(2)	2.23	0.38	-16.4	-11.9	8.9	1.340	0.670	0.670
C(6)–C(5)	2.17	0.43	-15.8	-11.1	8.9	1.353	0.676	0.676
C(5)–S(4)	1.26	0.20	-6.5	-5.4	3.5	1.792	0.902	0.890
C(3)–S(4)	1.33	0.21	-7.1	-5.8	3.4	1.766	0.901	0.865
C(6)–S(7)	1.27	0.20	-6.5	-5.4	3.5	1.792	0.902	0.890
C(8)–S(7)	1.33	0.21	-7.1	-5.8	3.4	1.766	0.865	0.901
C(8)–C(9)	2.23	0.38	-16.4	-11.9	8.9	1.340	0.670	0.670
C(6)–S(10)	1.26	0.20	-6.5	-5.4	3.5	1.792	0.890	0.902
C(9)–S(10)	1.33	0.21	-7.1	-5.8	3.4	1.766	0.865	0.901
C(2)–H(11)	1.87	0.02	-17.2	-16.8	9.0	1.059	0.703	0.357
C(3)–H(12)	1.87	0.02	-17.2	-16.8	9.0	1.059	0.703	0.357
C(8)–H(13)	1.87	0.02	-17.2	-16.8	9.0	1.059	0.357	0.703
C(9)–H(14)	1.87	0.02	-17.2	-16.8	9.0	1.059	0.357	0.703

Interestingly, the bond path analysis gives the better understanding of bond charge polarization effect of each bond's in the molecule; the C–C bonds are the very less polarized bonds, which is confirmed from the small bond critical point shift and the value is  $\sim 0.670\%$  (Figure 4). Bond polarization effects in C–S bonds are found considerably different, which confirms the bcp positions of these bonds are shifted mostly from the middle of the bonds at about 9%, near the respective carbon atoms; this amount of shift indicates that the charges of these bonds are highly polarized. Table 2, shows the bond charge polarization of the molecule, in which, the C–S bond is believed as the highly polarized bonds.

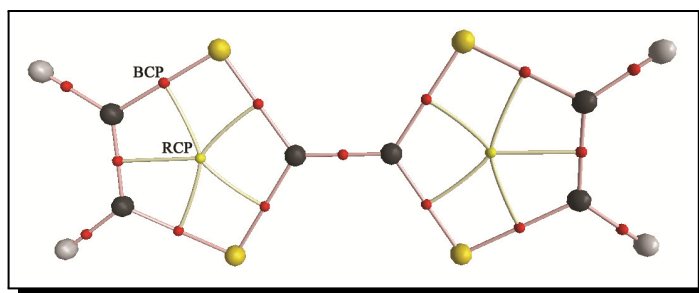


**Figure 4.** The molecular graph showing the (3, –1) and (3, –1) critical points of the TTF molecule. Big circle indicates the atomic positions, Small circle Red and Yellow indicates the bond and ring critical points, respectively

#### 4. Ionization Potential

The spatial redistribution of the frontier orbital is a three dimensional representation of local density of states which visually shows the electron density of the molecule [16]. Figure 5 illustrates the spatial redistribution of the molecular orbital for the various HOMO and LUMO orbital level of the molecule. The highest occupied molecular orbital HOMO, the lowest unoccupied molecular orbital (LUMO) are the frontier orbital's, the difference between them are known as HOMO–LUMO gap (HLG). HLG is one of the key factors determines the transport properties of the molecule [20, 24]. Large decrease in the HLG predicts the possibility of having reasonable conduction through the molecule, since, the conductivity increases with decreases in HLG [30]. Figure 6, shows the molecular orbital energy diagram of both methods. The calculated total molecular orbital energy for B3LYP/6-311G\*\* method is 3.75 eV, which is longer than the B3LYP/aug-cc-PVDZ calculations and the value is 3.63 eV. The value of HLG measured from these calculations is almost matching with the value calculated experimental methods [8].

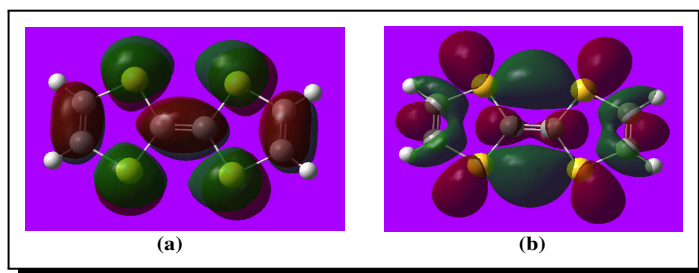


**Figure 5.** Isosurface representation of (a) Highest occupied molecular orbital (HOMO) (b) and Lowest unoccupied molecular orbital (LUMO) of TTF molecule

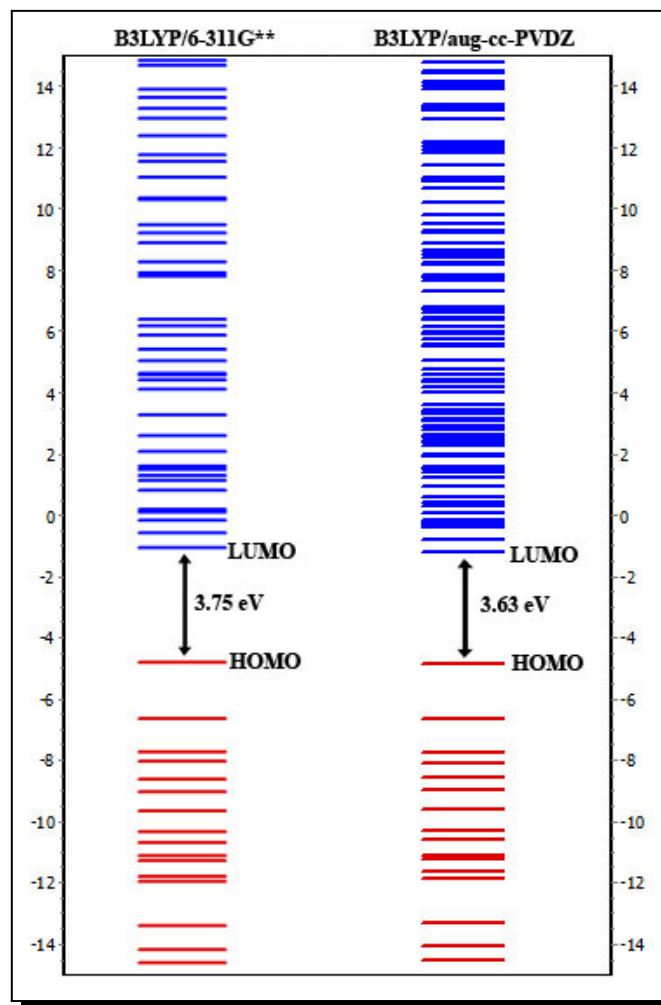


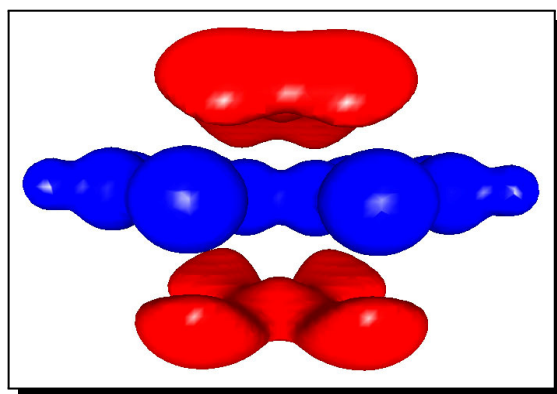
**Figure 6.** Molecular orbital energy level for B3LYP/6-311G\*\* and B3LYP/aug-cc-PVDZ calculations

## 5. MPA, NPA Charges and Electrostatic Potential

The information of charge distribution of the molecule is very much necessary to understand the molecular electrostatic potential, chemical reactivity and the electrostatic interactions [25]. Here, we report two kinds of charges, which are obtained from Mulliken population analysis (MPA) [18], Natural Population Analysis (NPA) [21] for to explore the ESP of the molecule. Table 3 gives the calculated atomic charges from different methods. Interestingly, mulliken population analysis are consistently higher than the natural Population analysis models charges. The C(2), C(3) and C(5) atoms MPA charges are found positive and the values is  $\sim 0.43$  e, further, the corresponding NPA charges is found negative ( $-0.41$ e); the dissimilarity between these two model charges are may be due to different method of atomic charge estimation in the molecule. The charge of S-atoms [S(1), S(4) and S(7), S(10)] are positive 0.06 (MPA) and 0.37 (NPA). The variation of charge between C and S atoms of this molecule implies that these bonds are highly polarized; seemingly, the bond charge polarization partly weakening the bond. Figure 7 shows the isosurface representation of electrostatic potential, the large negative ESP surface is found near S-regions, which gives the negative charge domination of the molecule.

**Table 3.** Atomic Charges of Tetrathiafulvalene (TTF) molecule

Atoms	MPA	NPA
S(1)	0.06	0.37
C(2)	0.43	-0.41
C(3)	0.43	-0.41
S(4)	0.06	0.37
C(5)	0.33	-0.44
C(6)	0.33	-0.44
S(7)	0.06	0.37
C(8)	0.43	-0.41
C(9)	0.43	-0.41
S(10)	0.06	0.37
H(11)	-0.65	0.26
H(12)	-0.65	0.26
H(13)	-0.65	0.26
H(14)	-0.65	0.26

**Figure 7.** Isosurface representation of electrostatic potential of Tetrathiafulvalene (TTF) molecule. Blue: positive potential ( $0.5 \text{ e}\text{\AA}^{-3}$ ), Red: negative potential ( $-0.5 \text{ e}\text{\AA}^{-3}$ )

## 6. Conclusion

The Structural and bond topological and electrostatic properties of TTF molecule have been studied using the DFT and charge density analysis. The optimized (B3LYP/6-311G\*\* and B3LYP/aug-cc-PVDZ) geometric parameters are in excellent agreement with the experimental data. The bond topological analysis based on the AIM theory shows the difference of charge distribution in all bonds. Notably, the less polarized bonds is C–C bond, which is confirmed from the small bcp shift of about less than 0.670%. The calculated total molecular orbital energy for B3LYP/6-311G\*\* method is 3.75 eV, which is longer than the B3LYP/aug-cc-PVDZ calculations and the value is 3.63 eV, these results gives the very good information of conductivity of the TTF molecule. These observations give an insight on this kind of super conducting material, which are useful to design navel electronic devices.

### Competing Interests

The authors declare that they have no competing interests.

## Authors' Contributions

All the authors contributed significantly in writing this article. The authors read and approved the final manuscript.

## References

- [1] R. F. W. Bader and T. T. Nguyen-Dang, Quantum theory of atoms in Molecules-Dalton revisited, *Adv. Quantum Chem.* **14** (1981), 63 – 124, DOI: 10.1016/S0065-3276(08)60326-3.
- [2] R. F. W. Bader, *Atoms in Molecule: A Quantum Theory*, Clarendon Press, Oxford, UK (1990).
- [3] R. F. W. Bader, Atoms in molecules, *Acc. Chem. Res.* **18** (1985), 9 – 15, DOI: 10.1021/ar00109a003.
- [4] M. R. Bryce, Recent progress on conducting organic charge-transfer salts, *Chem. Soc. Rev.* **20** (1991), 355, <https://pubs.rsc.org/en/content/articlelanding/1991/cs/cs9912000355/unauth#!divAbstract>
- [5] Y. C. Cheng, R. J. Silbey, D. A. da Silva Filho, J. P. Calbert, J. Cornil and J. L. Brédas, Three-dimensional band structure and bandlike mobility in oligoacene single crystals: A theoretical investigation, *J. Chem. Phys.* **118** (2003), 3764 – 3774. DOI: 10.1063/1.1539090.
- [6] C. D. Dimitrakopoulos and D. J. Mascaro, Organic thin-film transistors: A review of recent advances, *IBM J. Res. Dev.* **45** (2001), 11 – 27, <https://ieeexplore.ieee.org/document/5389079>.
- [7] E. Demiralp and A. W. Goddard, Structures and energetics study of tetrathiafulvalene-based donors of organic superconductors, *J. Phys. Chem. A* **101** (1997), 8128 – 8131, DOI: 10.1021/jp9716546.
- [8] E. Demiralp, W. A. Goddard, *Ab Initio* and semiempirical electronic structural studies on Bis(ethylenedithio)tetrathiafulvalene (BEDT-TTF or ET), *Journal of Physical Chemistry* **98** (1994), 9781 – 9785, <https://pubs.acs.org/doi/abs/10.1021/j100090a011?journalCode=jpchax>.
- [9] W.-Q. Deng and W. A. Goddard, Predictions of hole mobilities in oligoacene organic semiconductors from quantum mechanical calculations, *Journal of Physical Chemistry B* **108** (2004), 8614 – 8621, DOI: 10.1021/jp0495848.
- [10] M. J. Frisch, G. W. Trucks, H. B. Schlegel, G. E. Scuseria, M. A. Robb, J. R. Cheeseman, J. A. Montgomery, T. J. Vreven, K. N. Kudin, J. C. Burant, J. M. Millam, S. S. Iyengar, J. Tomasi, V. Barone, B. Mennucci, M. Cossi, G. Scalmani, N. Rega, G. A. Petersson, H. Nakatsuji, M. Hada, M. Ehara, K. Toyota, R. Fukuda, J. Hasegawa, M. Ishida, T. Nakajima, Y. Honda, O. Kitao, H. Nakai, M. Klene, X. Li, J. E. Knox, H. P. Hratchian, J. B. Cross, C. Adamo, J. Jaramillo, R. Gomperts, R. E. Stratmann, O. Yazyev, A. J. Austin, R. Cammi, C. Pomelli, J. W. Ochterski, P. Y. Ayala, K. Morokuma, G. A. Voth, P. Salvador, J. J. Dannenberg, V. G. Zakrzewski, S. Dapprich, A. D. Daniels, M. C. Strain, O. Farkas, D. K. Malick, A. D. Rabuck, K. Raghavachari, J. B. Foresman, J. V. Ortiz, Q. Cui, A. G. Baboul, S. Clifford, J. Cioslowski, B. B. Stefanov, G. Liu, A. Liashenko, P. Piskorz, I. Komaromi, R. L. Martin, D. J. Fox, T. Keith, M. A. Al-Laham, C. Y. Peng, A. Nanayakkara, M. Challacombe, P. M. W. Gill, B. Johnson, W. Chen, M. W. Wong, C. Gonzalez and J. A. Pople, *Gaussian03*, Gaussian, Inc., Pittsburgh, PA (2003).
- [11] D. Jerome, Superconductivity in a synthetic organic conductor (TMTSF)<sub>2</sub>PF<sub>6</sub>, *Journal of Physical Letters* **41** (1980), L95 – L98, DOI: 10.1051/jphyslet:0198000410409500.
- [12] T. A. Keith, AIMAll (Version 10.03.25), [aim.tkgristmill.com](http://aim.tkgristmill.com) (2010).
- [13] H. Klauk, M. Halik, U. Zschieschang, G. Schmid, W. Radlik and W. Weber, High-mobility polymer gate dielectric pentacene thin film transistors, *J. Appl. Phys.* **92** (2002), 5259, DOI: 10.1063/1.1511826.

- [14] H. Kobayashi, A. Kobayashi, S. Yukiyoishi, G. Saito and H. Inkuchi, Transverse conduction and metal-insulator transition in s-(BEDT-TTF)<sub>2</sub>PF<sub>6</sub>, *Bull. Chem. Soc. Jpn.* **59** (1986), 301.
- [15] W.A. Little, Superconductivity at room temperature, *Scientific American* **212** (1965), 21 – 27, DOI: 10.1038/scientificamerican0265-21.
- [16] R. J. Magyar, S. Tretiak, Y. Gao, H. L. Wang and A. P. Shreve, A joint theoretical and experimental study of phenylene–acetylene molecular wires, *Chemical Physical Letters* **401** (2005), 149 – 156, DOI: 10.1016/j.cplett.2004.10.155.
- [17] H. Mori, Overview of organic superconductors, *International Journal of Modern Physics B* **8**(1-2) (1994), 1 – 45, [https://inis.iaea.org/search/search.aspx?orig\\_q=RN:25057837](https://inis.iaea.org/search/search.aspx?orig_q=RN:25057837).
- [18] R. S. Mulliken, Electronic population analysis on LCAO–MO molecular wave functions. I, *Journal of Chemical Physics* **23** (1955), 1833, DOI: 10.1063/1.1740588.
- [19] J. P. Perdew, Density-functional approximation for the correlation energy of the inhomogeneous electron gas, *Phys. Rev. B* **33** (1986), 8822 – 8824, DOI: 10.1103/PhysRevB.33.8822.
- [20] D. F. Perepichka and M. R. Bryce, Molecules with exceptionally small HOMO-LUMO gaps, *Angew. Chem. Int. Ed.* **44** (2005), 5370 – 5373, DOI: 10.1002/anie.200500413.
- [21] A. E. Reed, L. A. Curtiss and F. Weinhold, Intermolecular interactions from a natural bond orbital, donor-acceptor viewpoint, *Chemical Reviews* **88** (1988), 899, DOI: 10.1021/cr00088a005.
- [22] G. Sato and Y. Yoshida, Development of conductive organic molecular assemblies: organic metals, superconductors, and exotic functional materials, *Bulltin Chemical Society of Japan* **80** (2007), 1, DOI: 10.1246/bcsj.80.1.
- [23] J. H. Schön, Ch. Kloc, R. C. Haddon and B. Batlogg, A superconducting field-effect switch, *Science* **288** (2000), 656 – 658, <http://science.sciencemag.org/content/288/5466/656>.
- [24] J. M. Seminario and Y. Liuming, Ab initio analysis of electron currents in thioalkanes, *International Journal of Quantum Chemistry* **102** (2005), 711 – 723, DOI: 10.1002/qua.20384.
- [25] P. Srinivasan, S. N. Asthana, R. B. Pawar and P. Kumaradhas, A theoretical charge density study on nitrogen-rich 4,4',5,5'-tetranitro-2,20-bi-1H-imidazole (TNBI) energetic molecule, *Structural Chemistry* **22** (2011), 1213 – 1220, [https://www.researchgate.net/publication/251220939\\_A\\_theoretical\\_charge\\_density\\_study\\_on\\_nitrogen-rich\\_44'55'-tetranitro-22'-bi-1H-imidazole\\_TNBI\\_energetic\\_molecule](https://www.researchgate.net/publication/251220939_A_theoretical_charge_density_study_on_nitrogen-rich_44'55'-tetranitro-22'-bi-1H-imidazole_TNBI_energetic_molecule).
- [26] A. D. Stephen, P. Srinivasan, S. N. Asthana, R. B. Pawar and P. Kumaradhas, Crystal structure prediction and charge density distribution of highly energetic dimethylnitraminotetrazole: a first step for the design of high energy density materials, *Central European Journal of Energetic Materials* **9**(3) (2012), 201 – 217, <http://www.wydawnictwa.ipowaw.pl/cejem/vol-9-3-2012/Stephen.pdf>.
- [27] S. V. Tsirelson, WinXPRO: a program for calculating crystal and molecular properties using multipole parameters of the electron density, *J. Appl. Cryst.* **35** (2002), 371 – 373.
- [28] A. Volkov, P. Macchi, L. J. Farrugia, C. Gatti, P. Mallinson, T. Richter and T. Koritsanszky, *XD2006 – a computer program for multipole refinement, topological analysis of charge densities and evaluation of intermolecular energies from experimental or theoretical structure factors*, version 5.33, State University of New York at Buffalo, NY; Università di Milano, Italy; University of Glasgow, UK; CNR-ISTM Milano, Italy; Free University of Berlin, Germany (2007), <http://xd.chem.buffalo.edu/docs/xd2006manual.pdf>.

- [29] Y. Yang, M. N. Weaver and K. M. Merz Jr., Assessment of the “6-31+G\*\* + LANL2DZ” mixed basis set coupled with density functional theory methods and the effective core potential: prediction of heats of formation and ionization potentials for first-row-transition-metal complexes, *J. Phys. Chem. A* **113** (2009), 9843 – 9851, <https://www.ncbi.nlm.nih.gov/pubmed/19691271>.
- [30] Y. Ye, M. Zhang and J. Zhao, *Ab initio* investigations on three isomers of polyacetylene under the interaction of the external electric field, *Journal of Molecular Structure (THEOCHEM)* **822** (2007), 12 – 20, DOI: 10.1016/j.theochem.2007.07.007.